The EMBO Journal (2011) 30, 945–958 | © 2011 European Molecular Biology Organization | All Rights Reserved 0261-4189/11
www.embojournal.org

THE EMBO JOURNAL

Polyglutamine Atrophin provokes neurodegeneration in *Drosophila* by repressing *fat*

Francesco Napoletano[1,4], Simona Occhi[1,4], Piera Calamita[1], Vera Volpi[2], Eric Blanc[2], Bernard Charroux[3], Julien Royet[3] and Manolis Fanto[1,2,*]

[1]Dulbecco Telethon Institute and Division of Neuroscience, DIBIT-San Raffaele Scientific Institute, Milan, Italy, [2]MRC Centre for Developmental Neurobiology, King's College London, Guy's Campus, London, UK and [3]IBDML, Campus de Luminy Case 907, Marseille Cedex 9, France

Large alterations in transcription accompany neurodegeneration in polyglutamine (polyQ) diseases. These pathologies manifest both general polyQ toxicity and mutant protein-specific effects. In this study, we report that the *fat* tumour suppressor gene mediates neurodegeneration induced by the polyQ protein Atrophin. We have monitored early transcriptional alterations in a *Drosophila* model of Dentatorubral-pallidoluysian Atrophy and found that polyQ Atrophins downregulate *fat*. Fat protects from neurodegeneration and Atrophin toxicity through the Hippo kinase cascade. Fat/Hippo signalling does not provoke neurodegeneration by stimulating overgrowth; rather, it alters the autophagic flux in photoreceptor neurons, thereby affecting cell homeostasis. Our data thus provide a crucial insight into the specific mechanism of a polyQ disease and reveal an unexpected neuroprotective role of the Fat/Hippo pathway.

The EMBO Journal (2011) **30,** 945–958. doi:10.1038/emboj.2011.1; Published online 28 January 2011
Subject Categories: neuroscience; molecular biology of disease
Keywords: *Atrophin*; autophagy; *fat*; Hippo pathway; neurodegeneration

Introduction

Polyglutamine (polyQ) diseases are a family of dominantly inherited neurodegenerative diseases, caused by an expanded CAG repeat tract resulting in polyQ stretches in the encoded protein (Ross, 2002).

For some time, the leading view in the field has been that the proteins affected by polyQ expansion misfold and accumulate in large aggregates, which are toxic for neurons and lead to cell death and organism pathology (Ross, 2002). However, this model has not been able to account for the striking cell-specific degeneration of polyQ diseases. More recent hypotheses hold that toxicity of polyQ proteins would be a mix of common intrinsic polyQ properties and specific negative effects given by the protein context, which would be responsible for the differences observed among various syndromes (Williams and Paulson, 2008).

It has been suggested in particular that polyQ diseases are transcriptionopathies in which toxicity first arises from large-scale alterations of transcription. These are major effects of polyQ toxicity and different models have been proposed to explain how they may arise (Wood *et al*, 2000; Nucifora *et al*, 2001; Luthi-Carter *et al*, 2002; Schaffar *et al*, 2004; Riley and Orr, 2006). In some cases it has been demonstrated that reinstating appropriate transcription factors can revert polyQ toxicity (Nucifora *et al*, 2001; Taylor *et al*, 2003). However, in most studies, it is difficult to sort out primary from secondary effects and thus whether transcriptional deregulation causes neurodegeneration or *vice versa*. In late-stage transcriptional analysis it is also harder to identify gene regulations linked to specific misfunctions of the proteins affected, rather than to common polyQ toxicity.

Dentatorubral-pallidoluysian Atrophy (DRPLA) is a human polyQ disease caused by the expansion of a CAG stretch in the *atrophin-1* (*at-1*) gene. In all vertebrates, a second *atrophin* gene, *at-2*, is present and encodes a related protein but void of polyQ tracts. Atrophins take part in several cellular processes and have been shown to function as bimodal transcriptional cofactors that are recruited to regulatory elements by a number of transcription factors (Wang *et al*, 2006; Shen *et al*, 2007).

Mouse knockouts exist for both *atrophin* genes, revealing that *at-2* has essential roles in the development of the nervous system, somites and limbs (Zoltewicz *et al*, 2004; Vilhais-Neto *et al*, 2010), whereas *at-1* is entirely redundant, possibly because a shorter form of At-2 (At-2S) may compensate for At-1 loss (Shen *et al*, 2007). Two different mouse models for DRPLA have been generated and both recapitulate important neurological and cytopathological features of human disease (Schilling *et al*, 1999; Sato *et al*, 2009). Major transcriptional alterations have been detected in DRPLA mice and these have also been compared with Huntington mouse models to reveal common alterations and also specific effects (Luthi-Carter *et al*, 2002; Sato *et al*, 2009).

In the fruitfly *Drosophila melanogaster* there is one conserved *Atrophin* (*Atro*) gene. Mutations in *Atro* reveal that it is required for diverse processes such as planar cell polarity and some forms of cell adhesion/cell affinities leading to defects in embryonic segmentation and leg and eye development (Erkner *et al*, 2002; Zhang *et al*, 2002; Fanto *et al*, 2003). Atro contains all functional domains of vertebrate atrophins, including two polyQ stretches, and is ubiquitously expressed. We have generated *Drosophila* models for DRPLA and described both polyQ and Atrophin-specific events that modulate cell and organism toxicity (Nisoli *et al*, 2010).

Because of the molecular function of Atrophins, DRPLA is a disease with a straightforward link to transcriptional

*Corresponding author. MRC Centre for Developmental Neurobiology, King's College London, Guy's Campus, London SE1 1UL, UK.
Tel.: +44 207 848 6807; Fax: +44 207 848 6550;
E-mail: manolis.fanto@kcl.ac.uk
[4]These authors contributed equally to this work and are listed in alphabetical order.

Received: 22 April 2010; accepted: 22 December 2010; published online: 28 January 2011

activity. To understand to what extent transcriptional alterations cause neurodegeneration and are linked to the normal functions of Atrophin, we carried out a genome-wide transcriptional profiling in our *Drosophila* models, focusing on primary events that precede neurodegeneration. Our data suggest that polyQ Atro causes metabolic stress and loss of terminal differentiation markers. Importantly, polyQ Atro represses transcription of the *fat* tumour suppressor gene, the function of which in this system protects from degeneration and Atrophin toxicity. In *fat* mutants, neurons undergo progressive degeneration with autophagic hallmarks. We also show that the Hippo pathway downstream of *fat* is necessary for correct neuronal homeostasis and mediates autophagic degeneration by Fat and polyQ Atrophins. Thus, our data uncover a specific mechanism of toxicity of a polyQ disease and reveal for the first time an unexpected neuroprotective role of the conserved Fat/Hippo tumour suppressor pathway.

Results

An experimental design aimed at early transcriptional responses to polyQ Atro

The eye is the most accessible part of the nervous system of the fly and is dispensable for life; therefore, it has been widely used to model neurodegeneration in *Drosophila*. To detect the earliest possible alterations in transcription resulting from the expression of polyQ Atro, we used a robust and reliable system to control the induction of expression (McGuire *et al*, 2004). Atro transgenes have been expressed in all retinal cells, using the combination of the *GMR–Gal4* driver with a temperature-sensitive mutant of the Gal80 repressor, expressed ubiquitously. When the flies are raised at 18°C, the transgenes are not expressed. Shifting the flies to 29°C results in Gal80 inactivation and Gal4-dependent transgene expression (Figure 1A).

Using this experimental design, expression of no transgene, wt Atro or two previously reported polyQ mutants, Atro66QC and Atro75QN (Nisoli *et al*, 2010), was induced. In all cases, RNA from whole heads has been isolated after 0, 2 and 14 days (d) of ageing at 29°C.

The first time point (in which flies are kept at 18°C) is a negative control for transgene expression to standardise possible differences in the genetic backgrounds. The other two time points have been selected on the basis of the extent of degeneration. After 2 days, no degeneration is detectable in the tangential eye section (Figure 1B). Minimal loss of photoreceptor neurons (~10% of the total) is present after 14 days in the retinae expressing the polyQ mutants (Figure 1B). However, if aged longer, flies expressing all forms of Atro develop more severe neurodegeneration with more dramatic vacuolisation, enhanced loss of the regular structure of the retinae, and, in the case of polyQ mutants, collapse of tissue (Supplementary Figure 1). Therefore, all Atro-overexpressing flies show signs of progressive degeneration, albeit at different speed.

Thus, this protocol focuses on early events in the neurodegenerative process and allows the characterisation of the initial transcriptional alteration, as the analysis terminates at a stage of degeneration that has often been the starting point in similar studies (Nelson *et al*, 2005).

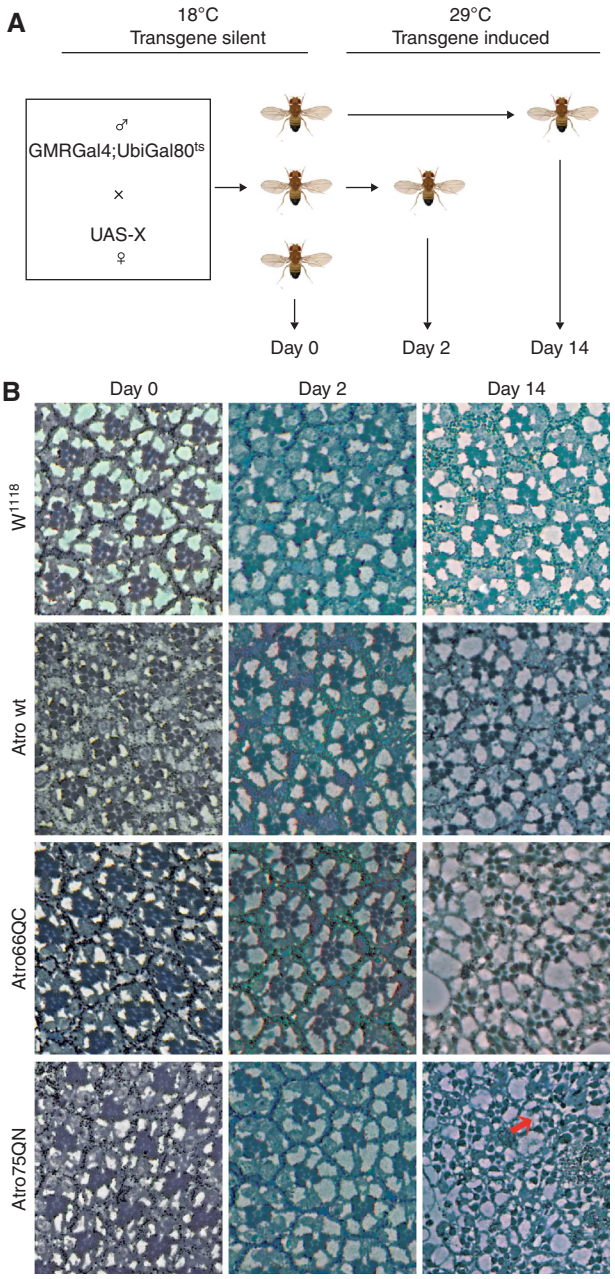

Figure 1 Transcriptional profiling of polyQ Atrophins. (**A**) Illustration of the crossing and ageing scheme used to obtain total RNA extracts from fly heads for the transcriptional profiling and all successive qPCR assays. Expression of different Atrophin forms with the *GMR* driver was induced, owing to a temperature-sensitive mutant Gal80 repressor. F1 flies were allowed to develop at 18°C; at this temperature the Gal80 repressor keeps transgenes silent. Newly eclosed flies (0–48 h) were collected and killed immediately (0d) or aged for 2 or 14 days at 29°C. This inactivates Gal80 and transgenes are switched on by *GMR-Gal4*. This protocol allows comparing siblings that differ exclusively in their age and transgenes expression. Control flies crossed to *GMR-Gal4; UbiGal80^{ts}* in all experiments are from the w^{1118} stock in which all UAS transgenes have been generated. (**B**) Tangential eye sections of flies representative of all the different populations used in the microarray analysis at all different time points. Weak degeneration is only visible after 14 days with polyQ Atro; in particular with Atro75QN there is an initial loss of photoreceptors (PR, arrow), 30.7% of the ommatidia has lost at least 1 PR, that is only 5.1% of all neuronal PR have been lost at this stage ($N = 333$).

Microarray analysis of transcriptional profiles and validation of results

Following *Drosophila* 2.0 Affymetrix arrays hybridisation and scanning, results were normalised and filtered. Data normalisation was carried out with two algorithms, RMA (Irizarry *et al*, 2003) and VSN (Huber *et al*, 2002). To focus on the impact of Atro mutations, all changes due to temperature shift and ageing, which are independent of Atro expression, were filtered out. No fold change threshold has been considered in our statistical filtering. Using this conservative protocol, 269 probe sets were called differentially expressed after 2 days in both normalisations, and 390 after 14 days. This indicates that a significant transcriptional response is set from very early on. The full list of detected alterations is shown in Supplementary Table 1.

Given the substantial agreement of both normalisation protocols, the more stringent VSN set was used for further global analysis. Most genes are downregulated by all forms of Atro, and the downregulating activity of polyQ Atro, but not of wt Atro, increases with time (Supplementary Figure 2). Within a given genotype, there are many changes over time, indicating significant progression in transcriptional responses despite marginal or no phenotypic alteration. Importantly, transcriptional response to Atro wt expression is stable between 2 and 14 days, whereas the polyQ mutants produced a more dynamic alteration, scattered in time, that suggests an intracellular conflict, resulting in opposed trends displayed over time by the same genes (Supplementary Figure 3).

Pattern clustering according to fold changes shows that the effects of the different Atro mutants branch mainly according to time points (Figure 2A and Supplementary Figure 4), matching phenotypic strength (Figure 1B and Supplementary Figure 1) and highlighting a convergent common polyQ effect. Venn diagrams (Figure 2B) illustrate that the degree of overlap between the different mutants increases

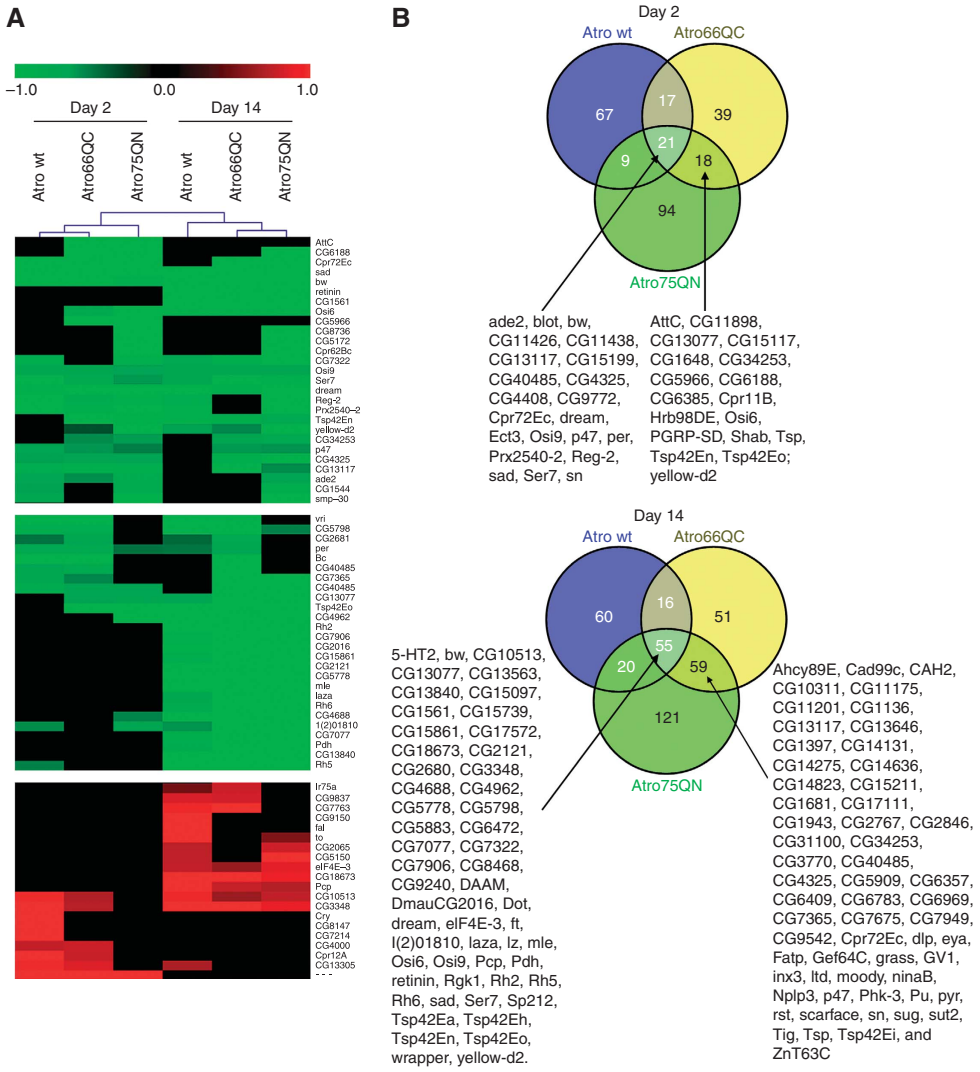

Figure 2 Global analysis of transcript profiling. (**A**) Heat maps for three subsets of the pattern clustering analysis generated using the Euclidean Distance metric. Upregulated genes are in red and downregulated genes are in green. The downregulating transcriptional activity increases with time. The main branch in clustering of the different Atro mutants is along time points. See also Supplementary Figure 4. (**B**) Venn diagrams for the subset of genes affected at the two time points for the different Atro versions with respect to control flies. The overlap between all Atro forms and the two polyQ versions increases with time. The genes in common for all Atro versions or between the polyQ Atro mutants at both times are listed.

with time, particularly between the two polyQ mutants. The increased convergence, however, appears to affect only the downregulated genes, whereas for upregulated genes the overlap remains constant (Supplementary Figure 5). We speculate that this may be because the downregulating activity rests on common properties of all Atro forms, whereas upregulation diverges more, perhaps because it reflects more indirect events. All these results are in agreement with the description of Atro as a corepressor (Erkner *et al*, 2002; Zhang *et al*, 2002; Haecker *et al*, 2007).

Gene ontology (GO) annotation and clustering of the probe sets carried out with the most commonly used tool, the DAVID 6.7 algorithm (Huang da *et al*, 2009), reveals that the vast majority of clusters deal with general metabolic processes, indicating a status of metabolic stress, the effects of which on neurodegeneration could be two-fold and will require further analysis (Supplementary Table 2 and Supplementary Figure 5).

Many genes affected are involved in the specialised function of phototransduction (cluster no. 2). These clusters are significantly altered by Atro75QN from the very early stages, whereas the effect of wt Atro is more delayed (Supplementary Table 2 and Supplementary Figure 5). Because our transcriptional profiling reflects events that take place well before severe degeneration (Figure 1B), these data do not result from cell and tissue loss. Rather, they suggest loss of terminal differentiation markers in photoreceptor neurons, which may result in early functional impairment.

Two other clusters include genes important for cell cycle and mitosis (nos. 27 and 40). This could result from either an attempt at cycle re-entry by post-mitotic neurons undergoing de-differentiation or compensatory proliferation by another cell population. Some clusters (nos. 34 and 38) are linked to programmed cell death (Supplementary Table 2 and Supplementary Figure 5), which appears to be repressed at the transcriptional level, as some key genes like the caspase *dream* are significantly downregulated (Supplementary Table 1).

We next focused on the set of genes commonly regulated by at least two Atro forms for validation of microarray data through two different qPCR approaches. Some genes were validated using standard real-time PCR and a larger scale confirmation was sought by analysing the pattern of expression of 17 genes with the Universal Probe Library approach, which couples qPCR with probe detection. We selected a spectrum of genes displaying different patterns and significance in the statistical analysis and in most cases the result of the qPCR confirmed the trend of the microarray analysis (Supplementary Figure 6). Interestingly, because of its greater sensitivity, this analysis revealed significant deregulation after 2 days as well and by wt Atro for some genes, including *fat (ft)*.

ft is transcriptionally regulated by Atrophins and is a direct target of Atro

The most intriguing single-gene alteration is the downregulation of the *ft* gene (Mahoney *et al*, 1991), a tumour suppressor that codes for a gigantic cadherin the cytoplasmic domain of which interacts with Atro to regulate planar polarity (Fanto *et al*, 2003). Real-time qPCR validated the microarry result for *ft* and further establishes the fact that wt Atro also significantly downregulates this gene, albeit at a much lower degree than the polyQ forms, which also affect this gene early on at 2 days (Figure 3A). Fat is an attractive candidate in light of the current knowledge on Atrophins. In addition, its multiple roles as a signalling molecule and cadherin link it potentially to many other processes highlighted in our analysis and make it of outstanding interest for further investigations.

The effect of wt Atro on *ft* suggests that its downregulation is linked to an Atrophin function, which is altered by polyQ expansion. In agreement with this hypothesis, downregulation of Atro by RNA interference leads to a significant upregulation of *ft* (Supplementary Figure 7). On the contrary, human Htt-exon-1, wt or with 93Q, does not affect *ft* transcription, indicating that this is not a common effect of polyQ proteins (Supplementary Figure 7).

Interestingly, overexpression of wt human Atrophin-1 upregulates *ft* (Supplementary Figure 7). This is consistent with the description of At-1 mainly as an activator of transcription (Shen *et al*, 2007) and its dominant-negative effects on Atro in flies (Charroux *et al*, 2006). However, polyQ expansion in At-1 interferes with the At-1 effect and downregulates *ft* with respect to control flies (Supplementary Figure 7). This suggests that the regulation of *ft* transcription is due to a conserved property of Atrophins and may be relevant to a human context as well.

To address whether Atro regulates *ft* transcription directly we carried out chromatin immunoprecipitation, followed by qPCR analysis of different regions that putatively regulate transcription immediately upstream of *ft* or in its first intron, in areas reported to be bound by RNA PolII in the modENCODE project (Celniker *et al*, 2009). In untreated S2 cells, we detected a mild but significant enrichment of a putative enhancer region 3.9 kb upstream of the *ft* transcriptional start site (Supplementary Figure 7). To confirm this result in a neuronal context and to establish its dependence on the levels of Atro, we used a clone of BG3 *Drosophila* neuronal cells. These cells express low levels of Atro endogenously and have been previously validated by us for the pathological response to polyQ Atro (Nisoli *et al*, 2010). We have stably transfected BG3 cells with exogenous Atro under inducible control and, although we were unable to select a pure clonal population, we enriched the transfected fraction of the population up to 70% by antibiotic selection. ChIP from induced cell extracts detected a specific and statistically significant enrichment of the −3.9 kb region of the *ft* promoter, in comparison with uninduced cells (Figure 3B). This confirms that Atro interacts in ChIP experiments with this region, and that increasing the levels of *Atro* increases the amount of Atro protein that interacts with this enhancer. These data indicate that *ft* is a direct target of Atro and strongly support the hypothesis that its downregulation results from a direct activity of Atro on a specific enhancer region upstream of *ft*.

ft mediates Atro neurodegeneration and is required for neuronal homeostasis

To address the functional significance of *ft* downregulation for neurodegeneration induced by Atrophins, we tested genetic interactions in *Drosophila* between the two mutants. Two independent and molecularly characterised (Matakatsu and Blair, 2006) loss of function alleles of *ft* (ft^{fd} and ft^{Grv}) in heterozygosis enhance photoreceptor loss due to Atro75QN expression with *Rhodopsin-1-Gal4* (Figure 3C). When wt or

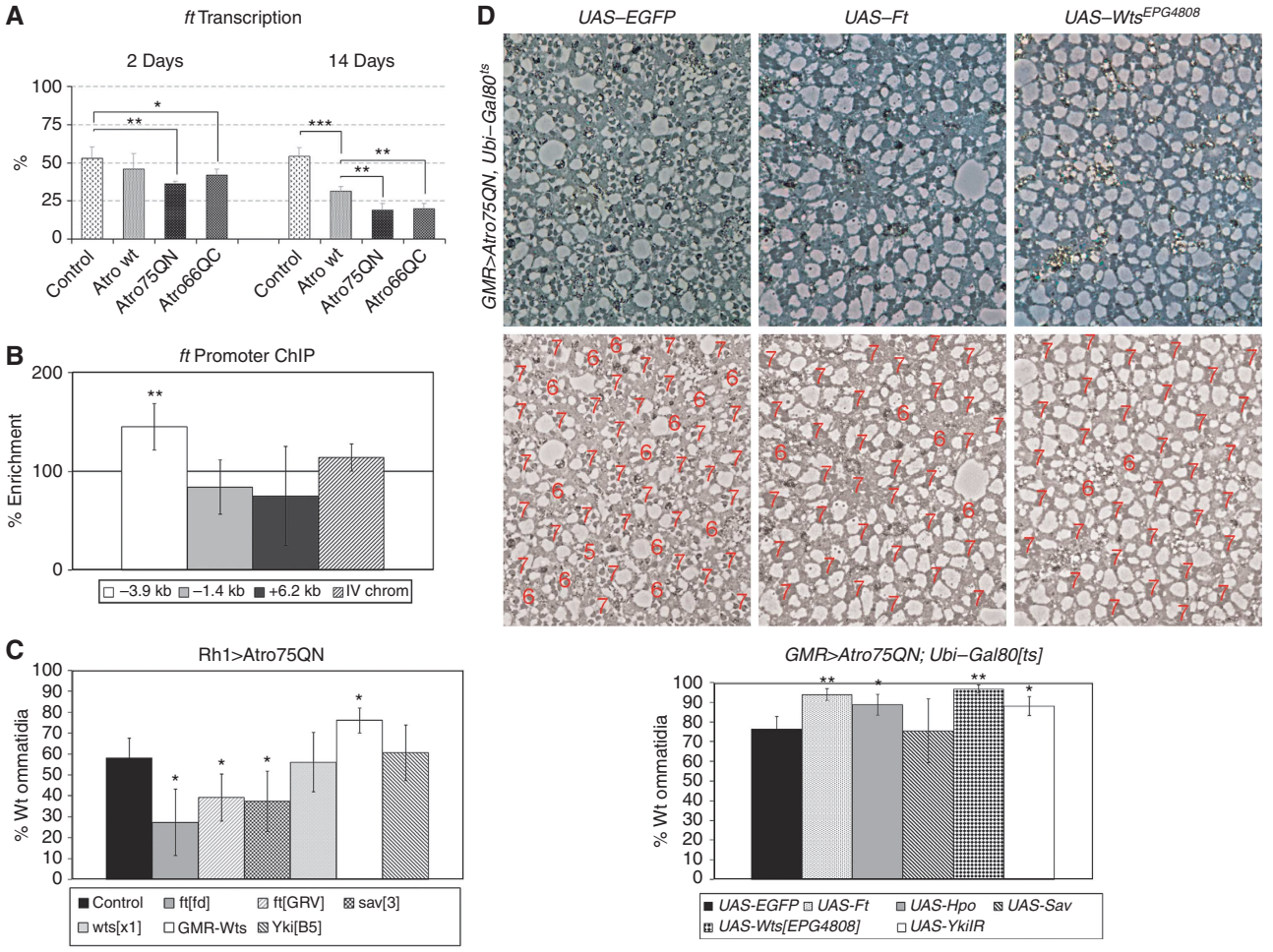

Figure 3 Regulation of *ft/Hpo* levels is functionally relevant to neurodegeneration by Atrophins. Statistical significance is marked as follows: $***P<0.001$, $**P<0.01$; $*P<0.05$ in two-tailed *t*-test. All qPCR results here and in all figures are the average of three reactions of independent biological replicas. (**A**) qPCR analysis of the fold changes ± s.d. of *ft* transcription. Downregulation starts at 2 days and progresses at 14 days. (**B**) qPCR analysis of the enrichment ± s.d. of different regions of the *ft* regulatory elements in ChIP for Atro from BG3 neuronal cell extracts. Enrichment is calculated as the percentage of DNA immunoprecipitated from extracts of cells in which Atro expression has been induced, with respect to the amount immunoprecipitated from uninduced cell extracts according to the $(\text{Atro–No Ab})_{\text{induced}}/(\text{Atro}-\text{No Ab})_{\text{uninduced}}$ formula. The DNA region from IV chromosome has been previously shown not to be immunoprecipitated in ChIP for Atro (Haecker *et al*, 2007) and has been used as a negative control. (**C**) Histograms showing the number of ommatidia with a full complement (7) of PR in flies expressing Atro75QN with the *Rhodopsin1* driver in either a control (w^{1118}) or different mutant backgrounds and aged at 29°C for 28 days. Heterozygosis for two independent *ft* alleles and a *sav* allele significantly enhances the loss of PR. Mild overexpression of Wts via a *GMR–wts* transgene, which does not display any strong phenotype *per se*, significantly suppresses the loss of PR. No interaction was detected in this assay with wts^{x1} and yki^{B5} alleles in heterozygosity. $N=430–963$ from at least four eyes. (**D**) Tangential eye sections and histograms showing the degeneration of *GMR>Atro75QN, Ubi–Gal80^{ts}* flies in combination with different UAS transgenes and aged 14 days as in Figure 1A. *UAS–EGFP* is used as a negative control. Either Ft or Wts overexpression strongly suppresses loss of PR caused by Atro75QN. Lower panels are provided as examples of quantification. A more modest but still significant rescue is observed by overexpressing a Yki RNAi contruct or Hpo; however, in this case it is to be considered that the overexpression of Hpo *per se* brings about the loss of at least one PR in ∼5% of ommatidia (data not shown). No effect is detected with overexpression of Sav. Two-tailed *t*-test: $*P<0.05$; $**P<0.01$. The $wts^{EPG4808}$ is a previously uncharacterised EP element insertion at the 5′ of the *wts* gene. Rare homozygous escapers display larger eyes, whereas in combination with *GMR–Gal4* this line gives rise to smaller rough eyes, and, finally, qPCR analysis of *GMR>*$wts^{EPG4808}$ indicates a 10-fold increase in the head content of *wts* mRNA (data not shown).

polyQ Atro is expressed with *GMR–Gal4*, the retina collapses progressively (Nisoli *et al*, 2010) and this is enhanced by heterozygosis for ft^{fd} (Supplementary Figure 8). On the contrary, overexpression of an exogenous Ft construct leads to significant suppression of neuronal cell loss, retinal collapse and premature organism lethality, which arises when polyQ Atrophins are expressed in glial cells with *RepoGal4* (Nisoli *et al*, 2010; Figure 3D and Supplementary Figure 8). These results indicate that regulation of *ft* levels is functionally relevant for Atrophin-mediated neurodegeneration, also outside the context of retinal neurons.

This suggests that *ft* itself may be required for neuronal homeostasis. Strikingly, homozygous mutant clones for ft^{fd} in the eye bring about progressive retinal degeneration when the flies are aged through our standard protocol. Although the *ft* mutant tissue is normal after eclosion from the pupal case, photoreceptors start degenerating in aged flies and finally the whole *ft* mutant tissue falls apart (Figure 4A). A quantification of the severity of the degeneration shows significant and remarkable progression with age (Figure 4B). A similar, albeit weaker, phenotype is displayed by another independent *ft* allele, ft^{82}, but not by a *wt* clone (Supplementary Figure 9). To

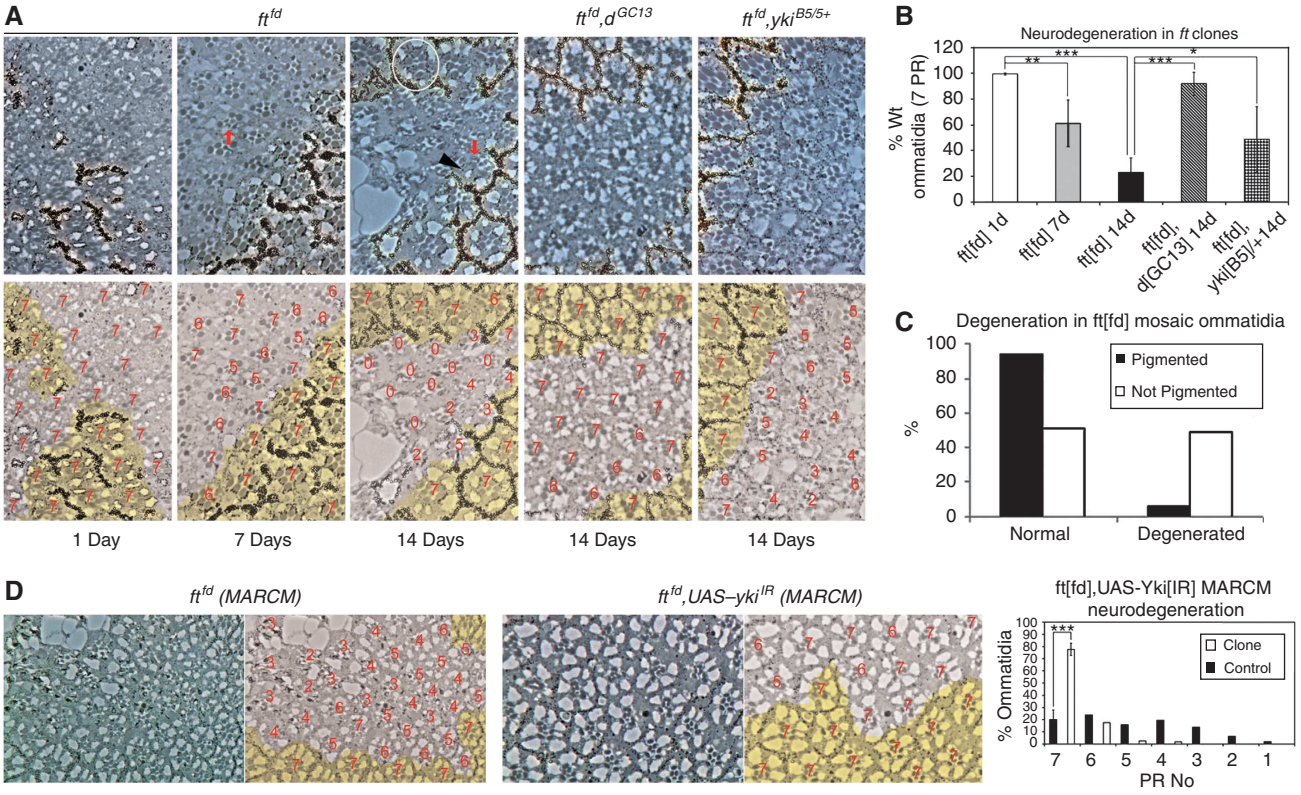

Figure 4 Neurodegeneration by mutations in *ft*. (**A**) Tangential eye sections through ft^{fd} clones aged 1, 7 and 14 days, of ft^{fd},d^{DGC13} double mutant clones and of ft^{fd} clones in a yki^{B5} heterozygous background aged 14 days. Clones are marked by the absence of yellow pigment. Arrows point at degenerating photoreceptors, arrowheads point at intact wt photoreceptors in mosaic ommatidia. The circled ommatidium is genetically *wt* but non-autonomously flipped in its polarity and has not degenerated. Lower panels are masks that show clonal borders and quantification of PR number per ommatidia. After 14 days, almost all ft^{fd} cells have degenerated, whereas almost all ft^{fd},d^{DGC13} and some $ft^{fd},yki^{B5/+}$ neuronal photoreceptors have not. (**B**) Histograms showing the quantification of degeneration in ft^{fd}, $ft^{fd}d^{DGC13}$ and $ft^{fd}yki^{B5/+}$ clones. Loss of *ft* leads to statistically significant loss of neurons and this is suppressed at 14 days by $yki^{B5}$and much more dramatically by d^{DGC13}. $^{***}P<0.001$, $^{**}P<0.01$; $^{*}P<0.05$ in two-tailed *t*-test. (**C**) Degeneration in mosaic ommatidia in ft^{fd} clones. At this stage of degeneration approximately half of the non-pigmented (genotypically mutant) PR cells display a degenerative phenotype, whereas virtually all pigmented (genotypically *wt*) PR cells are normal. χ^2-test: 82.38; $P<0.001$. Total PR $N=310$ (pigmented) and 327 (not pigmented). (**D**) Tangential eye sections through MARCM clone mutants for ft^{fd} that express either no transgene or an RNAi construct against *yki* ($UAS–yki^{IR}$) with *Tub–Gal4* and aged 14 days at 29°C. Because the transgene $UAS–yki^{IR}$ is on chromosomal arm 2 L, the same as *ft*, clones generated with this system carry two copies of $UAS–yki^{IR}$ and therefore downregulate *yki* very effectively. No other cell outside the clones expresses the construct and is therefore wt for *yki*. Mask panel is presented on the right of each section. A quantification of photoreceptor numbers (far right) displays a very significant increase in the number of wt ommatidia ($N=210$ and 219 from four eyes). $^{***}P<0.001$ in two-tailed *t*-test. If all classes of ommatidia are considered, χ^2-test = 232.30; $P<0.001$ for 3 degrees of freedom.

assess whether the temperature used (29°C) in the ageing protocol made a critical contribution to the emergence of neuronal degeneration, ft^{fd} clones were aged at 25°C. At this temperature, neurodegeneration in *ft* clones progresses more slowly on an absolute time scale (Supplementary Figure 9). However, if the difference in lifespan at the two temperatures is taken into consideration (14 days represent 40% of the mean survival for *wt* flies at 29°C, whereas 21 days at 25°C represent 33.3% of mean survival), neurodegeneration due to lack of *ft* at 25°C is as strong as, if not stronger than, at 29°C.

Mitotic clones are generated during larval development; this raises the possibility that *ft* mutations may lead neurons to degenerate through an effect in development. To address whether loss of *ft* specifically in adult post-mitotic cells is sufficient to cause neurodegeneration, an RNAi construct against *ft* was expressed in the adult photoreceptors with *GMRGal4* and $Gal80^{ts}$, as for the transcriptional profiling. Also in this case, photoreceptor cells are progressively and significantly lost (Supplementary Figure 10) despite a completely normal development of the retina. The effect of the RNAi is much weaker than that of mutant clones and does not entirely rule out a contribution of developmental abnormalities to the neurodegeneration observed in *ft* mutant clones. Given the weak efficacy of this RNAi line (as judged by the mild polarity phenotypes recovered when expressed in development, data not shown), this limited effect could be expected; however, this result indicates that Ft is also required specifically in adult neurons for their homeostasis.

Ft is a multifunctional protein that takes part in several cellular processes and many hypotheses could be put forward as to the mechanism through which it affects neuronal survival. A first possibility is that the Ft planar polarity pathway, in which Atro is also involved, could mediate neurodegeneration. However, genetically *wt* ommatidia outside the clones, the polarity of which is non-autonomously affected by neighbouring *ft* mutant cells, are not susceptible to degeneration (Figure 4A). In addition, at a stage of neurodegeneration in which half of *ft* mutant cells (not

pigmented) are degenerating in mosaic ommatidia, the neighbouring *wt* cells (pigmented) are almost totally unaffected (Figure 4C). This analysis reveals that degeneration by loss of *ft* is strictly cell autonomous, in contrast to the *ft* planar polarity phenotypes (Fanto *et al*, 2003).

Ft is also a cadherin that can putatively affect cell adhesion, and loss of cell contacts could potentially lead to degeneration. However, electron microscopy (EM) analysis reveals that adherent junctions are preserved in cells at an advanced degeneration stage (Supplementary Figure 11), indicating that loss of cell adhesion is not driving degeneration. In addition, driving an RNAi transgene against *shotgun* (coding for the fly E-cadherin), specifically in the adult retina through the Gal4/Gal80^{ts} system, leads to disorganisation of the distribution of pigment cells and orientation of the ommatidia but not to degeneration or loss of neurons (Supplementary Figure 11). Thus, it is unlikely that loss of a potential role of Ft in cell adhesion would be required for the degenerative phenotype.

The Hippo tumour suppressor pathway controls neurodegeneration

It has been shown that Ft controls tissue growth and proliferation cell autonomously through the Hippo tumour suppressor pathway, although the phenotype of *ft* mutants does not entirely overlap with those of the other components of the pathway (Harvey and Tapon, 2007). We analysed the possibility that the Hippo pathway mediates neurodegeneration and, in agreement with this hypothesis, homozygous mutant clones for the core components of the pathway (Tapon *et al*, 2002), *warts* (*wts*), *salvador* (*sav*) and *hippo* (*hpo*), display significant progressive neuronal photoreceptor degeneration (Figure 5 and Supplementary Figure 12) very similar to that of *ft*.

In mutants of the Hippo pathway there is also a massive overgrowth of lattice cells, which results in increased ommatidial spacing as previously described (Tapon *et al*, 2002). Lattice cells are also sensitive to ageing and, despite appearing intact in newly enclosed flies, they rapidly degenerate, leading to dramatic tissue collapse (Figure 5 and Supplementary Figure 12).

The Hippo cascade represses the transcriptional co-activator Yorkie (Yki; Huang *et al*, 2005). Overexpression of Yki in flip-on clones, which causes loss of Hippo signalling, also brings about progressive neuronal degeneration (Supplementary Figure 13), albeit at a much weaker level if compared with loss of *ft* or of the *hippo* core genes.

To address whether Hippo signalling is required specifically in adult neurons for its neuroprotective function, as is the case for *ft*, we expressed Yki in adult retinae only with *GMR–Gal4* and *Gal80^{ts}* and detected unequivocal, albeit weak, neuronal cell loss (Figure 6A and B).

These data establish that the Hippo pathway is required for cell homeostasis specifically in adult neurons.

The Hippo pathway partially mediates neurodegeneration by ft and polyQ–Atro

Our analysis so far suggests the hypothesis that neurodegeneration by loss of *ft* and overexpression of Atro is therefore mediated by the Hippo pathway. It has been shown that Ft regulates the Hippo cascade through repression of the unconventional myosin Dachs, a negative regulator of the

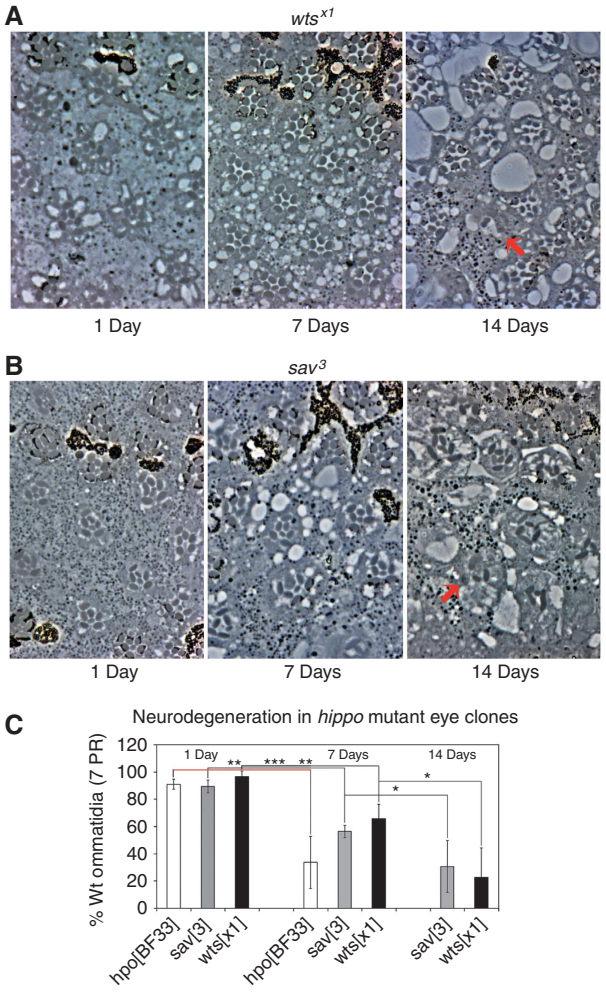

Figure 5 Neurodegeneration by mutations in Hippo pathway genes. All Hippo pathway mutant clones display a remarkable increase in interommatidial space as a consequence of failure in lattice programmed cell death and these lattice cells also degenerate with age (see also Supplementary Figure 12). Arrows point at degenerating neuronal photoreceptor cells. (**A**) Tangential eye sections through *wts^{X1}* mutant fly eyes. In clones for the null *wts^{X1}* allele, degeneration inside the clones is at severe stages at 14 days. (**B**) Tangential eye sections through *sav^{3}* clones. In *sav^{3}* after enclosure many photoreceptors are intact but after 14 days at 29°C most *sav* mutant photoreceptors have degenerated. (**C**) Histograms showing the quantification of ommatidia with the full complement of photoreceptors in *hpo*, *wts* and *sav* mutant clones. The progression of loss of photoreceptors is evident and statistically significant in all cases. Mutants for *hpo^{BF33}* do not survive for 14 days at 29°C and corresponding sections are shown in Supplementary Figure 12. $N = 195–268$. $^{***}P < 0.001$, $^{**}P < 0.01$; $^{*}P < 0.05$ in two-tailed *t*-test.

pathway (Cho *et al*, 2006). Consistent with our hypothesis, mutations in *dachs (d)* strikingly rescue neurodegeneration due to loss of *ft* (Figure 4A and B). *d* single mutant clones remain wt (Supplementary Figure 12), as expected by the fact that Dachs is inhibited by Ft (Cho *et al*, 2006), and therefore its loss of function mimics Ft activation rather than loss.

Heterozygous mutations for *yki* also suppress the degeneration inside *ft* mutant clones (Figure 4A and B). Despite statistical significance, the weak rescue did not allow a complete assessment of the role of Yki in this pathway, which was also questioned by the weaker phenotypes

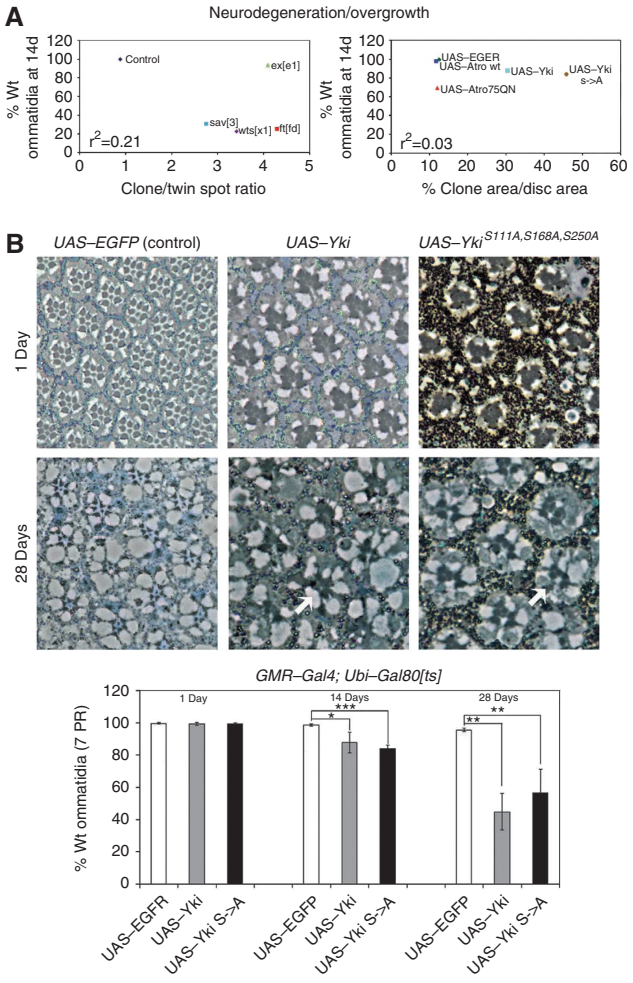

Figure 6 Uncoupling of neurodegeneration and overgrowth. (**A**) Regression analysis of the overgrowth versus the neurodegeneration observed in loss of function mutants (left) and overexpression of transgenes (right). Overgrowth quantification is shown in Supplementary Figure 14. For loss of function mutant, the neurodegeneration was quantified at 14 days in clones (as shown in Figures 4 and 5). For UAS-overexpression transgenes neurodegeneration was quantified at 14 days when expressed with *GMRGal4; UbiGal80^{ts}*. For CycD + Cdk4, these specific data are missing and have not been plotted; however, Supplementary Figure 13 shows that these mutants do not cause neurodegeneration in a different setup in which they are expressed during both development and adult life. In both cases the regression coefficient r^2 is extremely low (0.21 and 0.03), indicating an absence of correlation between the two processes. (**B**) Tangential eye sections through the eyes of flies expressing with *GMR–Gal4, Ubi–Gal80^{ts}* either *UAS*–EGFP or UAS–*Yki* or *UAS–Yki^{S111A,S168A,S250A}* and aged 1 or 28 days. Arrows point at missing or degenerated photoreceptors. The *UAS–Yki^{S111A,S168A,S250A}* is so effective that even the very low expression leaking out with this system is enough to affect development and generate mild eye roughness and overproliferation of lattice cells. Histograms showing the quantification of cell loss in eyes shown in A and also eyes from flies aged at the intermediate 14-day stage. Mild but significant degeneration is observed for both Yki forms, with respect to the negative control; however, no statistical difference is observed between the two Yki proteins that have dramatically different effects on overgrowth. $^{***}P<0.001$, $^{**}P<0.01$; $^{*}P<0.05$ in two-tailed *t*-test.

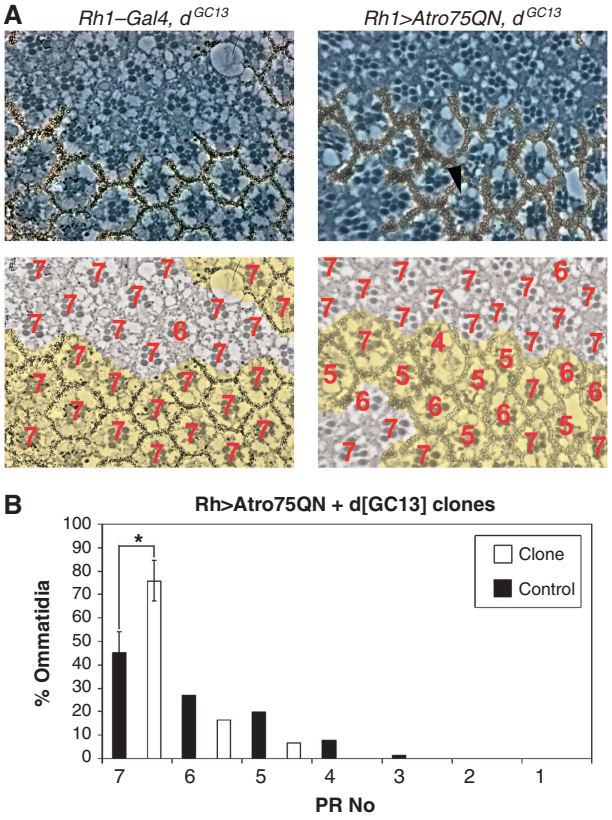

Figure 7 Neurodegeneration by polyQ Atro partially requires *dachs*. Tangential eye sections through d^{GC13} clones (marked by the absence of yellow pigment) either in control flies or those expressing Atro75QN with the *Rhodopsin1* driver and aged 28 days. Mask panels below each section exemplify clonal boundaries and PR no. for the ommatidia. Early signs of degeneration indicated by reduced complement of photoreceptors are detected specifically in the pigmented area (arrowhead). At this stage, inside *d* mutant clones all ommatidia are unaffected and display a *wt* arrangement (arrows). (**B**) Histograms showing the quantification of cell loss in eyes shown in (**A**). A statistically significant rescue is obtained both for the number of wt ommatidia ($^{*}P<0.05$ in two-tailed *t*-test) and for all other categories of ommatidia ($\chi^2=44.76$; $P<0.001$ for 2 degrees of freedom).

obtained through Yki overexpression. To further dissect the *ft–yki* interaction we took advantage of the MARCM technique (Lee and Luo, 2001) to express with *Tub–Gal4* an RNAi construct against Yki specifically inside *ft* clones. These experiments established that downregulation of *yki* dramatically suppressed the neurodegenerative phenotype due to loss of *ft* (Figure 4D).

As polyQ Atro overexpression results in downregulation of *ft* at the transcriptional level, and *ft* mediates part of the Atro toxicity, the Ft/Hippo pathway may also be required for polyQ Atro. Importantly, neuronal photoreceptor degeneration by Atro75QN is significantly suppressed inside *d* clones (Figure 7), indicating that the *d*-dependent branch of the Ft pathway mediates part of the polyQ Atro degeneration.

Furthermore, mild Gal4-independent expression of *wts* suppresses neurodegeneration brought about by expression of Atro75QN with *Rh-1–Gal4* (Figure 3C), whereas heterozygosity for *sav* enhances it. Heterozygosity for *yki* or *wts* did not display an effect in this particular setup; however, Gal4-dependent overexpression of Wts, through an EP element insertion, or Hpo or an RNAi against *yki*, suppressed the degenerative phenotype caused by adult expression of Atro75QN in the retina with *GMR–Gal4* and *Gal80^{ts}*

(Figure 3D and Supplementary Figure 8). In particular the effect of Wts was dramatic and comparable to the rescue caused by Ft overexpression.

Taken together, these data establish that the Hippo pathway mediates neurodegeneration due to loss of *ft* and, at least partially, also the degeneration caused by polyQ Atro expression.

Neurodegeneration is not a secondary effect of overproliferation

The Hippo pathway is a well-known tumour suppressor pathway that controls organ size in *Drosophila* and mammals (Harvey and Tapon, 2007). It may be hypothesised that neurodegeneration could arise as a secondary consequence of excessive proliferation or as a stimulus for neurons to re-enter the cell cycle, as also suggested by a set of data in the microarray analysis. We thus set out to tackle this possible mechanism for neurodegeneration. Stimulating growth and cell cycle independently of the Hippo signalling by over-expression of CyclinD in combination with Cyclin-dependent-kinase 4 (Datar *et al*, 2000) did not bring about any significant cellular degeneration (Supplementary Figure 13). Likewise, mutant clones for *expanded*, a tumour suppressor gene linked through multiple mechanisms to the Hippo pathway (Feng and Irvine, 2007; Badouel *et al*, 2009) that is however outside the pathway core and does not recapitulate all *hippo* pathway mutant phenotypes (e.g., lattice cells excess), caused overgrowth but no discernible loss of neurons even after 21 days at 29°C (Supplementary Figure 12). These two experiments suggest that effective overgrowth during development does not necessarily result in adult neurodegeneration.

In contrast, the most complete phosphomutant Yki ($Yki^{S111A,S168A,S250A}$), which cannot be inactivated by Wts (Oh and Irvine, 2009), brings about dramatic overproliferation and significant loss of adult photoreceptor neurons (Supplementary Figure 13). However, the malformation of the tissue and the altered recruitment of photoreceptors into clusters, present as a result of incorrect development, make it difficult to compare the effect of this mutant with that of the wt Yki protein. When expressed specifically in adult retina, however, $Yki^{S111A,S168A,S250A}$ causes significant but weak neurodegeneration, indistinguishable from the one caused by wt Yki (Figure 6B). This indicates that the function of Yki (and of the Hippo pathway) in adult neuronal homeostasis can be separated by that in proliferation and does not appear to be affected through phosphorylation of those residues known to be critical in proliferation.

This conclusion applies to all other mutants, as no correlation can be observed between the degree of overgrowth caused by several different loss of function or overexpressing mutants in the eye imaginal discs and the degree of neurodegeneration observed in the same neuroepithelium in adult stages (Figure 6A and Supplementary Figure 14).

It is in particular worth noting that Atro75QN does not cause any significant overgrowth. BrdU incorporation experiments confirm that expression of this polyQ protein drives some cells into cell cycle re-entry and DNA replication, as suggested by the microarray analysis; however, these are exclusively non-neuronal cells (Supplementary Figure 15).

In conclusion, these results indicate that overgrowth and neurodegeneration are not similarly affected and rule out excessive developmental proliferation and cell cycle re-entry as the mechanism through which Atro, Fat and the Hippo pathway affect neuronal degeneration.

Ft and Hippo components cause neurodegeneration through defective autophagy

We have previously reported that neurodegeneration due to polyQ–Atro arises through defective autophagy (Nisoli *et al*, 2010) and the Hippo pathway has been shown to affect autophagy during salivary gland degradation (Dutta and Baehrecke, 2008). Therefore, we also sought to establish the contribution of this cellular mechanism for neurodegeneration caused by loss of the Ft/Hippo signalling pathway.

EM analysis of *ft* mutant photoreceptors reveals autophagic vacuoles filled with unstructured partially degraded material and mitochondrial damage inside mutant photoreceptors (Figure 8A). Autophagosomes accumulate moderately but significantly with age in *ft* mutant neurons, in comparison with *wt* neurons (Figure 8B). Staining for GFP::Atg8a, a marker for autophagosomes, confirms the presence of these organelles in *ft* mutant cells (Figure 8C), in agreement with the EM analysis. The p62 protein, a multifunctional scaffold protein that marks ubiquitinated protein aggregates destined to autophagic degradation (Bjorkoy *et al*, 2005; Nezis *et al*, 2008), accumulates specifically inside *ft* mutant cells early on and increases dramatically with the progression of degeneration (Figure 8D). In addition, as already reported in the case of polyQ Atro (Nisoli *et al*, 2010), block of autophagy induction via mutations in *atg1* results in stronger or faster degeneration, as clones double mutant for *ft* and *atg1* are more degenerated than *ft* clones at the same age (Supplementary Figure 16) and *atg1* single mutants are wt at this stage.

Finally, EM analysis of *sav* mutant cells reveals a statistically significant accumulation of autophagic vesicles with partially degraded content identical to the vesicles detected in *ft* mutants (Figure 9A and B). Taken together, these data indicate that mutations in *ft* and the Hippo pathway genes deregulate autophagy in photoreceptor neurons and that autophagy is functionally relevant to neurodegeneration, as already shown for polyQ Atro (Nisoli *et al*, 2010).

Discussion

Polyglutamine diseases have been proposed to be 'transcriptionopathies' and transcriptional alterations are a major effect of polyQ toxicity (Riley and Orr, 2006). However, in most cases, it is difficult to sort out primary from secondary effects and thus whether transcriptional deregulation causes neurodegeneration or *vice versa*. We designed an experimental setup to unequivocally establish the chain of events by taking advantage of an effective inducible system of expression and analysing early time points at which no or very little degeneration is present. The mild phenotypes guarantee that detected alterations are caused neither by massive cell loss nor by severe degeneration; rather, they are early events that precede, and may give rise to, neurodegeneration.

Our results demonstrate conclusively the presence of robust transcriptional alterations from very early phases and that some of these alterations progress to later stages and are functionally relevant to neurodegeneration, like in

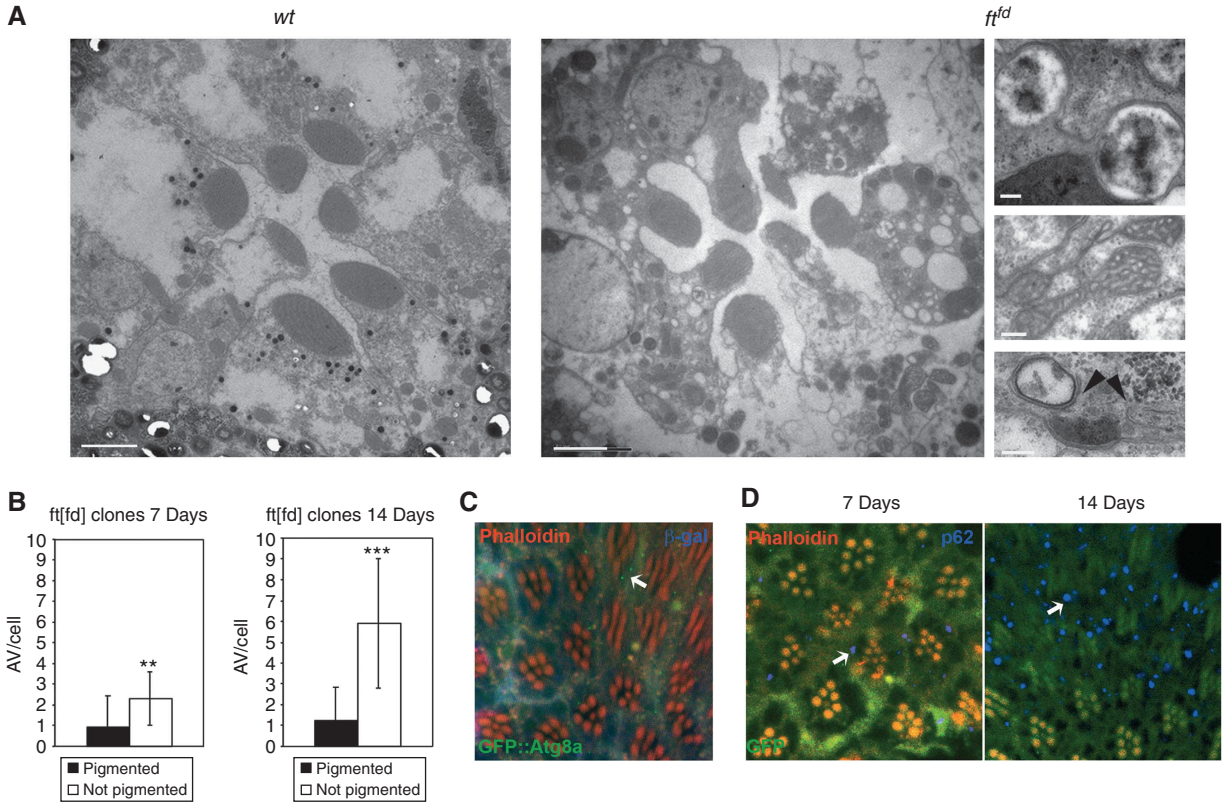

Figure 8 Autophagic modifications in *ft* mutants. (**A**) EM scan of a *wt* (left) and ft^{fd} mutant ommatidium (right) of a ft^{fd} clone after 14 days. Scale bar: 1 μm. High-magnification panels (far right, top to bottom) display autophagosomes with undigested debris, damaged mitochondria and forming phagophores (arrowheads), found in ft^{fd} mutant cells. Scale bar: 0.2 μm for zoom-in panels. (**B**) Graphs of the quantification of autophagic vesicles (AV) per photoreceptor found in EM sections of 7-day (left)- and 14-day (right)-old ft^{fd} clones. Significant accumulation of AV is found in mutant cells (not pigmented) with respect to genotypically wt (pigmented) cells. $^{**}P<0.01$ and $^{***}P<0.001$ in one-tailed *t*-test. $N=12$ pigmented cells versus 20 non-pigmented cells for the 7-day graph and 13 pigmented cells versus 21 non-pigmented cells for the 14-day graph. (**C**) Confocal pictures of whole-mount retinae of a ft^{fd} clone aged 7 days and expressing GFP::Atg8a ubiquitously with *Tub–Gal4*. Red is phalloidin marking rhabdomeres, green is GFP and the clone is marked by the absence of β-gal staining (blue). Small GFP::Atg8a dots accumulate specifically inside *ft* mutant cells (arrow). (**D**) Confocal pictures of whole-mount retinae of a ft^{fd} clone aged 7 days (left) and 14 days (right). Red is phalloidin marking rhabdomeres, blue is p62 and the clone is marked by the absence of GFP staining (green). p62 starts to gather in small dots specifically inside *ft* mutant cells (arrow) and then accumulates massively (arrow) in the *ft* mutant clones as many cells degenerate.

the case of *ft*. Although a time-course analysis cannot identify whether transcriptional changes are a result of direct Atrophin function or indirect events, the genes affected early on, also by wt Atro, are more likely to be linked to direct Atrophin transcriptional regulation, as is the case for *ft*, whereas genes affected only later on are more likely to be indirect responses to ongoing processes in the cell.

Global scale analysis of alterations leads to three major conclusions. First, the activity of Atro and its polyQ mutants is mostly a repressive one, in agreement with the corepressor function attributed to Atro (Erkner *et al*, 2002; Zhang *et al*, 2002; Haecker *et al*, 2007). Second, the polyQ effect builds a significant share of its toxicity upon an existing Atro toxicity by altering the transcription of genes affected by wt Atro as well. This confirms at a genome-wide level previous conclusions drawn from genetic and phenotypic examination (Nisoli *et al*, 2010) and is in agreement with recent discoveries that also link polyQ expansion to gain of normal protein functions (Duvick *et al*, 2010; Nedelsky *et al*, 2010). Third, functional clustering analysis revealed a complex set of transcriptional alterations, which hint at many different components: some, like oxidative and metabolic stress, commonly found in polyQ toxicity or retinal degeneration in *Drosophila* (Xu *et al*, 2004; Nelson *et al*, 2005), others previously unreported, like loss of terminal differentiation markers linked to the specialised phototransduction process. Importantly, we also do not find evidence of induction of apoptosis by Atrophin at the transcriptional level, which is quite the opposite, as some key genes are significantly downregulated.

The different approaches, neuronal tissues and statistical treatments used make it difficult to compare our result with that of previous transcriptional profiling in DRPLA mouse models (Luthi-Carter *et al*, 2002; Sato *et al*, 2009). A detailed comparison has also not been attempted between the two mouse models. However, we find some commonalities in the prevalence of downregulations, and the marked effects on metabolism and signal transduction.

Although over 80% of the candidate genes have been confirmed by qPCR, the few negative results, which include highly statistically significant candidates, stress the requirement for independent validation of functional genomic data before drawing conclusions about biological relevance. Thus, it is fundamental to establish whether such transcriptional

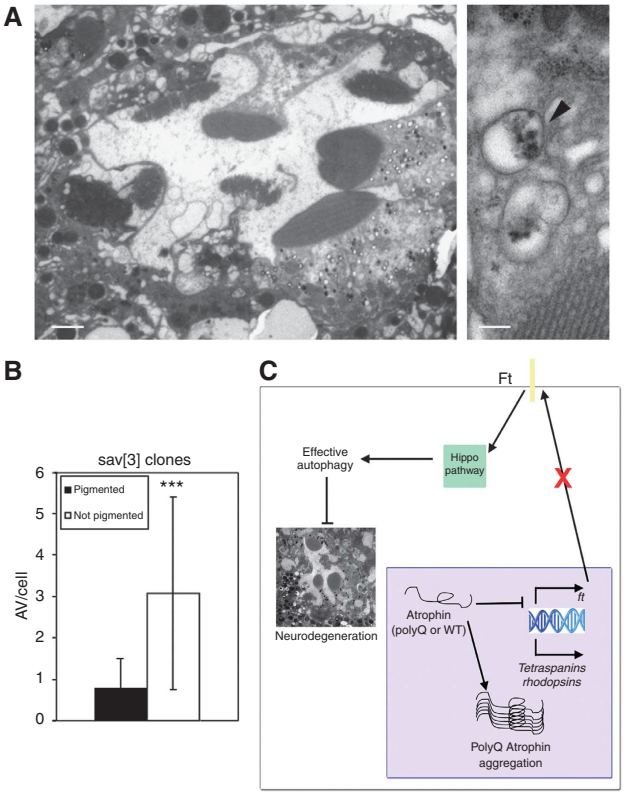

Figure 9 Autophagy in *sav* mutants. (**A**) EM scan of a 7-day-old *sav*^{3} mutant ommatidium and zoom-in on autophagosomes containing undigested debris (arrowhead). Scale bar: 1 μm for panel on the left and 0.2 μm for zoom-in panel on the right. (**B**) Graph of the quantification of autophagic vesicles (AV) per photoreceptor found in EM sections of 1-week-old *sav*^{3} clones. Significant accumulation of AV is found in mutant cells. ***$P<0.001$ in one-tailed *t*-test. $N=45$ pigmented cells versus 42 non-pigmented cells. (**C**) Model for the relationship between Atro, Ft/Hippo and neuronal homeostasis. Atro wt overexpression, and more effectively polyQ Atro overexpression, causes a downregulation of *ft* transcription and of other genes important for photoreceptor neuron function and homeostasis. This results in downregulation of Ft/Hippo signalling, which affects neurodegeneration. Healthy Ft/Hippo signalling contributes to neuronal homeostasis through effective autophagy. Atro may also exert Ft-independent effects through other factors (like Tetraspanins) and polyQ Atro also affects neurons through polyQ-specific factors (like misfolding and aggregation), which put additional pressure on the autophagic system. Other polyQ proteins may not feed into the Ft/Hippo pathway, as in the case of Htt-ex1-93Q in flies.

alterations are mere covariants or are functionally relevant for polyQ–Atro-driven neurodegeneration. Our attention has been attracted by the regulation of tumour suppressor *ft* as the best candidate for further analysis on the basis of the current biological knowledge of Ft and Atrophins in multiple model systems. In this study, we establish that neurodegeneration in our DRPLA model is partially mediated by loss of Ft expression, which is a direct target of Atro, downregulated at the transcriptional level. Because mutations in *Atro* phenocopy mutations in *ft* in ommatidial polarity (Fanto *et al*, 2003), and overexpressed Atro (also with polyQ expansion) acts as a gain of function in planar polarity and wing vein establishment (data not shown), transcriptional downregulation of *ft* represents a negative feedback loop in Ft/Atro signalling rather than the main pathway stream.

Despite different effects of the wt forms of fly and human Atrophins on *ft* transcription, which are consistent with the differences in proteins structure and with their known effects on transcription (Zhang *et al*, 2002; Wang *et al*, 2006; Shen *et al*, 2007), in both cases polyQ expansion results in potentially toxic downregulation of *ft*. This mechanism is, however, not a general property of all polyQ proteins; rather, it is specific for Atrophin toxicity, as indicated by the absence of any effect of a Huntingtin mutant on *ft*. The basis of this is likely to rely on Atro directly regulating the *ft* gene, as we show that Atro is recruited to a specific enhancer region 3.9 kb upstream of the *ft* transcriptional start site and increased *Atro* levels lead to increased Atro recruitment at the site. As Atro does not bind DNA directly, it must be recruited by a currently unknown transcription factor. This will be the subject of further investigations in the future.

Although polyQ Atrophins, as polyQ proteins, also elicit many detrimental effects that are not dependent on Ft, like misfolding and aggregation (Nisoli *et al*, 2010), part of their toxicity is accomplished through an alteration of the Ft/Hippo signalling cascade that we identify as a crucial pathway for post-mitotic cellular homeostasis. In the context of DRPLA, the role of *ft* downregulation is to be considered as a modulatory event, specifically due to the Atrophin protein context, which is added to the many other polyQ toxic effects (Figure 9C).

A straightforward hypothesis would be that neurodegeneration in *ft/hippo* mutants arises as a consequence of apoptosis inhibition and growth stimulation, which would put the cells under considerable metabolic stress. Downregulation of Ft/Hippo signalling may push neuronal cells to attempt re-entering cell cycle, known to be a detrimental event in other neurodegenerative conditions (Herrup and Yang, 2007). This may be consistent with some of our microarray results, which report a repression of apoptosis and a moderate stimulation of cell proliferation; however, both categories are only mildly enriched in GO clustering and we demonstrate that cell cycle re-entry, as visualised by BrdU incorporation, only affects non-neuronal cells and is therefore to be interpreted as compensatory proliferation, probably linked to an attempt at tissue repair and scar formation.

Furthermore, we demonstrate that the effects on overgrowth and on neuronal homeostasis of the different Hippo pathway components are clearly uncoupled. This is exemplified by the strikingly different effects on proliferation and neurodegeneration achieved by Yki in its wt or phosphomutant form. Whereas Yki^{S111A,S168A,S250A} has an effect on proliferation that is dramatically stronger than its wt counterpart, in adult post-mitotic neurons it achieves the same level of neurodegeneration as Yki wt.

In addition, the most effective polyQ Atro mutant, Atro75QN, does not cause any overgrowth, and transcription of the canonical targets of Ft/Hippo/Yki in growth control, like *cyclin-E* and *diap1*, is not altered in our model.

In conclusion, our data do not support a mechanism that links overgrowth to neurodegeneration and suggest that the Hippo pathway may work through a different mechanism and different targets in adult neurons.

The Hippo pathway has also been shown to regulate growth-unrelated events in post-mitotic neurons (Mikeladze-Dvali *et al*, 2005; Emoto *et al*, 2006) and in the retina Wts

regulates the correct Rhodopsin expression in R7/R8 cells (Mikeladze-Dvali *et al*, 2005) independently of growth regulation. It has also been recently shown that mutations in the Hippo pathway block induction of autophagy in the digestion of salivary glands during pupal stages, independently of Yki (Berry and Baehrecke, 2007; Martin *et al*, 2007; Dutta and Baehrecke, 2008). The alteration of autophagy is an attractive alternative cellular mechanism through which the Ft/Hippo pathway could mediate Atrophin toxicity. We previously reported that polyQ Atro induces neurodegeneration through a critical block in the autophagic flux (Nisoli *et al*, 2010). Interestingly Atro, also called Gug, has also been identified as a molecule important for autophagic digestion of salivary glands (Martin *et al*, 2007).

Our data also confirm the role of Hippo signalling in regulating autophagy. Indeed, the effect of Hippo signalling in autophagic cell death of the salivary glands is consistent with our observations, with some remarkable difference. We note unequivocal accumulation of autophagosomes in *ft* and *sav* mutant cells. This suggests that the block in adult neurons is in clearance, rather than in induction, of autophagic vacuoles as it is in the salivary glands (Dutta and Baehrecke, 2008). The discrepancy is also likely to reflect the different role and basal level of autophagy in the two tissues. Whereas in the salivary glands autophagy is massively induced as a cell killing mechanism, in post-mitotic neurons expressing polyQ Atrophins autophagy is a rescue attempt, which fails because of a block at the level of lysosomal digestion (Nisoli *et al*, 2010). The double mutant *ft,atg1* clones support the protective nature of endogenous levels of autophagy, also for *ft*-induced degeneration.

In addition, although more weakly than *ft* or other Hippo pathway components, Yki is capable of phenocopying neurodegeneration and its downregulation is able to suppress degeneration caused by loss of *ft*. The effects of *yki* in the retina could be due to a fundamental difference with salivary glands and are best interpreted by a model in which Yki is necessary but not sufficient to mediate all the functions of Hippo signalling in neuronal homeostasis, differently from growth control.

The data reported in this study suggest that degeneration by *ft* is due to autophagic stress and phenocopies many, but not all, aspects of polyQ Atrophin toxicity. The effect of *ft* mutations is more similar to the overexpression of wt Atro, in which, as in *ft*, at the ultrastructural level there is accumulation of autophagosomes but not of massive undigested autophagolysosomes (Nisoli *et al*, 2010). In addition, overexpression of wt Atro, as for loss of *ft*, leads to considerable accumulation of p62 with little increase in Atg8 punctae, whereas polyQ versions of Atrophins induce a much greater accumulation of Atg8. This would be consistent with a model (Figure 8C) in which Ft mediates an Atrophin-specific part of the toxicity, distinct from the general polyQ toxicity (i.e. protein misfolding, aggregation and resulting metabolic stress), and yet significantly affected by polyQ expansion in Atro.

The detailed molecular mechanism through which Ft and the Hippo pathway affect autophagy awaits further investigations, both in the context of development and in post-mitotic adult neurons. Nevertheless, it is likely that any effect on autophagy by the Ft pathway would be of crucial importance for its role in tumour suppression as well, given the relevance of autophagy in tumours and the wealth of common mechanisms shared by cancer and ageing (Finkel *et al*, 2007).

Finally, at least four Ft orthologues have been identified in mammals and are widely expressed throughout the mouse CNS (Tanoue and Takeichi, 2005), and Ft-1 has recently been shown to interact with mouse Atrophins (Hou and Sibinga, 2009), indicating an evolutionarily conserved relation. Transcriptional profiling analyses on DRPLA mouse models (Luthi-Carter *et al*, 2002; Sato *et al*, 2009) have not detected downregulation in any of the *ft* mouse genes. However, the array platform used in both studies (Affymetrix Mu 11K) did not include any mouse *ft*. It is thus possible that the regulation of Ft-like molecules and of the Hippo tumour suppressor cascade in mammals is important for neuroprotection and has a key role in DRPLA in humans.

Materials and methods

Genetics

The following mutant fly stocks have been used: *dEAAT1-Gal4, GMR-Gal4, Rhodopsin1-Gal4, Repo-Gal4, Tub-Gal4, GMR>w^{+}>Gal4, UAS-EGFP, UAS-Ft, UAS-Hpo, UAS-Sav, UAS-Wts^{EPG4808}, UAS-Yki, UAS-Yki^{S111A,S168A,S250A}, UAS-Yki^{IR}, UAS-CycD, UAS-Cdk4, UAS-GFP::Atg8a, Ubi-Gal80^{ts}, Tub-Gal80, ft^{fd},ft^{82}, ft^{Grv}yki^{B5}, atg1$^{\Delta 3D}$, d^{GC13}, sav^{3}, hpo^{BF33}, wts^{X1}* and *wts^{MGH1}*. All clones have been generated with the Flp/FRT system using either *ey-flp* or *hs-flp*.

Histology and EM

Semithin retinal sections were obtained as previously reported (Montrasio *et al*, 2007). EM samples were processed as in Nisoli *et al*, 2010.

Immunohistochemistry

Immunostaining procedures of adult retina were carried out with whole-mount preparation as previously reported (Nisoli *et al*, 2010). The following antibodies were used: mouse anti-β-galactosidase (1:1000) (Promega), rabbit anti-GFP (1:500, Molecular Probe), rabbit anti-p62 (1:2000) (a gift from Didier Contamine), mouse anti-Elav (1:500) (DHSB) and rat anti-BrdU (1:100) (AbCam). Secondary fluorescence-conjugated antibodies from Molecular Probes or Jackson Laboratories were used at 1:200 dilutions. Samples were viewed with BioRad and Zeiss LSM confocal microscopes.

The microarray data set is available at GEO (www.ncbi.nlm.nih.gov/geo/) with the accession ID: GSE26246. See Supplementary data for further Materials and methods.

Supplementary data

Supplementary data are available at *The EMBO Journal* Online (http://www.embojournal.org).

Acknowledgements

We thank Hugo Stocker, Nic Tapon, Tor Erik Rusten, Thomas Neufeld, Didier Contamine, the DHSB, VDRC and the Bloomington stock centre for reagents and stocks; Jean Paul Chauvin for technical assistance with EM; Tomi Ivacevic and Vladimir Benes for Microarray hybridisation; Larry Wrabetz, Guy Tear and Ivo Lieberam for critical reading of the paper. A very special thanks to Chi-Cheng Tsai for the gift of the anti-Atro Ab. MF was supported by the Italian Telethon Foundation with a career development award and was an Assistant Telethon Scientist. This work was also supported by the EU Marie Curie European Reintegration Grant 505739, by Fondazione Cariplo (2004-1527) and funds from the KCL School of Biomedical Sciences to MF.

Conflict of interest

The authors declare that they have no conflict of interest.

References

Badouel C, Gardano L, Amin N, Garg A, Rosenfeld R, Le Bihan T, McNeill H (2009) The FERM-domain protein expanded regulates Hippo pathway activity via direct interactions with the transcriptional activator Yorkie. *Dev Cell* **16:** 411–420

Berry DL, Baehrecke EH (2007) Growth arrest and autophagy are required for salivary gland cell degradation in Drosophila. *Cell* **131:** 1137–1148

Bjorkoy G, Lamark T, Brech A, Outzen H, Perander M, Overvatn A, Stenmark H, Johansen T (2005) p62/SQSTM1 forms protein aggregates degraded by autophagy and has a protective effect on huntingtin-induced cell death. *J Cell Biol* **171:** 603–614

Celniker SE, Dillon LA, Gerstein MB, Gunsalus KC, Henikoff S, Karpen GH, Kellis M, Lai EC, Lieb JD, MacAlpine DM, Micklem G, Piano F, Snyder M, Stein L, White KP, Waterston RH (2009) Unlocking the secrets of the genome. *Nature* **459:** 927–930

Charroux B, Freeman M, Kerridge S, Baonza A (2006) Atrophin contributes to the negative regulation of epidermal growth factor receptor signaling in Drosophila. *Dev Biol* **291:** 278–290

Cho E, Feng Y, Rauskolb C, Maitra S, Fehon R, Irvine KD (2006) Delineation of a Fat tumor suppressor pathway. *Nat Genet* **38:** 1142–1150

Datar SA, Jacobs HW, de la Cruz AF, Lehner CF, Edgar BA (2000) The Drosophila cyclin D-Cdk4 complex promotes cellular growth. *EMBO J* **19:** 4543–4554

Dutta S, Baehrecke EH (2008) Warts is required for PI3K-regulated growth arrest, autophagy, and autophagic cell death in Drosophila. *Curr Biol* **18:** 1466–1475

Duvick L, Barnes J, Ebner B, Agrawal S, Andresen M, Lim J, Giesler GJ, Zoghbi HY, Orr HT (2010) SCA1-like disease in mice expressing wild-type ataxin-1 with a serine to aspartic acid replacement at residue 776. *Neuron* **67:** 929–935

Emoto K, Parrish JZ, Jan LY, Jan YN (2006) The tumour suppressor Hippo acts with the NDR kinases in dendritic tiling and maintenance. *Nature* **443:** 210–213

Erkner A, Roure A, Charroux B, Delaage M, Holway N, Core N, Vola C, Angelats C, Pages F, Fasano L, Kerridge S (2002) Grunge, related to human Atrophin-like proteins, has multiple functions in Drosophila development. *Development* **129:** 1119–1129

Fanto M, Clayton L, Meredith J, Hardiman K, Charroux B, Kerridge S, McNeill H (2003) The tumor-suppressor and cell adhesion molecule Fat controls planar polarity via physical interactions with Atrophin, a transcriptional co-repressor. *Development* **130:** 763–774

Feng Y, Irvine KD (2007) Fat and expanded act in parallel to regulate growth through warts. *Proc Natl Acad Sci USA* **104:** 20362–20367

Finkel T, Serrano M, Blasco MA (2007) The common biology of cancer and ageing. *Nature* **448:** 767–774

Haecker A, Qi D, Lilja T, Moussian B, Andrioli LP, Luschnig S, Mannervik M (2007) Drosophila brakeless interacts with atrophin and is required for tailless-mediated transcriptional repression in early embryos. *PLoS Biol* **5:** e145

Harvey K, Tapon N (2007) The Salvador-Warts-Hippo pathway—an emerging tumour-suppressor network. *Nat Rev Cancer* **7:** 182–191

Herrup K, Yang Y (2007) Cell cycle regulation in the postmitotic neuron: oxymoron or new biology? *Nat Rev Neurosci* **8:** 368–378

Hou R, Sibinga NE (2009) Atrophin proteins interact with the Fat1 cadherin and regulate migration and orientation in vascular smooth muscle cells. *J Biol Chem* **284:** 6955–6965

Huang J, Wu S, Barrera J, Matthews K, Pan D (2005) The Hippo signaling pathway coordinately regulates cell proliferation and apoptosis by inactivating Yorkie, the Drosophila Homolog of YAP. *Cell* **122:** 421–434

Huang da W, Sherman BT, Lempicki RA (2009) Systematic and integrative analysis of large gene lists using DAVID bioinformatics resources. *Nat Protoc* **4:** 44–57

Huber W, von Heydebreck A, Sultmann H, Poustka A, Vingron M (2002) Variance stabilization applied to microarray data calibration and to the quantification of differential expression. *Bioinformatics* **18**(Suppl 1)**:** S96–S104

Irizarry RA, Hobbs B, Collin F, Beazer-Barclay YD, Antonellis KJ, Scherf U, Speed TP (2003) Exploration, normalization, and summaries of high density oligonucleotide array probe level data. *Biostatistics* **4:** 249–264

Lee T, Luo L (2001) Mosaic analysis with a repressible cell marker (MARCM) for Drosophila neural development. *Trends Neurosci* **24:** 251–254

Luthi-Carter R, Strand AD, Hanson SA, Kooperberg C, Schilling G, La Spada AR, Merry DE, Young AB, Ross CA, Borchelt DR, Olson JM (2002) Polyglutamine and transcription: gene expression changes shared by DRPLA and Huntington's disease mouse models reveal context-independent effects. *Hum Mol Genet* **11:** 1927–1937

Mahoney PA, Weber U, Onofrechuk P, Biessmann H, Bryant PJ, Goodman CS (1991) The fat tumor suppressor gene in Drosophila encodes a novel member of the cadherin gene superfamily. *Cell* **67:** 853–868

Martin DN, Balgley B, Dutta S, Chen J, Rudnick P, Cranford J, Kantartzis S, DeVoe DL, Lee C, Baehrecke EH (2007) Proteomic analysis of steroid-triggered autophagic programmed cell death during Drosophila development. *Cell Death Differ* **14:** 916–923

Matakatsu H, Blair SS (2006) Separating the adhesive and signaling functions of the Fat and Dachsous protocadherins. *Development* **133:** 2315–2324

McGuire SE, Mao Z, Davis RL (2004) Spatiotemporal gene expression targeting with the TARGET and gene-switch systems in Drosophila. *Sci STKE* **2004:** pl6

Mikeladze-Dvali T, Wernet MF, Pistillo D, Mazzoni EO, Teleman AA, Chen YW, Cohen S, Desplan C (2005) The growth regulators warts/lats and melted interact in a bistable loop to specify opposite fates in Drosophila R8 photoreceptors. *Cell* **122:** 775–787

Montrasio S, Mlodzik M, Fanto M (2007) A new allele uncovers the role of echinus in the control of ommatidial rotation in the Drosophila eye. *Dev Dyn* **236:** 2936–2942

Nedelsky NB, Pennuto M, Smith RB, Palazzolo I, Moore J, Nie Z, Neale G, Taylor JP (2010) Native functions of the androgen receptor are essential to pathogenesis in a Drosophila model of spinobulbar muscular atrophy. *Neuron* **67:** 936–952

Nelson B, Nishimura S, Kanuka H, Kuranaga E, Inoue M, Hori G, Nakahara H, Miura M (2005) Isolation of gene sets affected specifically by polyglutamine expression: implication of the TOR signaling pathway in neurodegeneration. *Cell Death Differ* **12:** 1115–1123

Nezis IP, Simonsen A, Sagona AP, Finley K, Gaumer S, Contamine D, Rusten TE, Stenmark H, Brech A (2008) Ref(2)P, the *Drosophila melanogaster* homologue of mammalian p62, is required for the formation of protein aggregates in adult brain. *J Cell Biol* **180:** 1065–1071

Nisoli I, Chauvin JP, Napoletano F, Calamita P, Zanin V, Fanto M, Charroux B (2010) Neurodegeneration by polyglutamine Atrophin is not rescued by induction of autophagy. *Cell Death Differ* **17:** 1577–1587

Nucifora Jr FC, Sasaki M, Peters MF, Huang H, Cooper JK, Yamada M, Takahashi H, Tsuji S, Troncoso J, Dawson VL, Dawson TM, Ross CA (2001) Interference by huntingtin and atrophin-1 with cbp-mediated transcription leading to cellular toxicity. *Science* **291:** 2423–2428

Oh H, Irvine KD (2009) *In vivo* analysis of Yorkie phosphorylation sites. *Oncogene* **28:** 1916–1927

Riley BE, Orr HT (2006) Polyglutamine neurodegenerative diseases and regulation of transcription: assembling the puzzle. *Genes Dev* **20:** 2183–2192

Ross CA (2002) Polyglutamine pathogenesis: emergence of unifying mechanisms for Huntington's disease and related disorders. *Neuron* **35:** 819–822

Sato T, Miura M, Yamada M, Yoshida T, Wood JD, Yazawa I, Masuda M, Suzuki T, Shin RM, Yau HJ, Liu FC, Shimohata T, Onodera O, Ross CA, Katsuki M, Takahashi H, Kano M, Aosaki T, Tsuji S (2009) Severe neurological phenotypes of Q129 DRPLA transgenic mice serendipitously created by en masse expansion of CAG repeats in Q76 DRPLA mice. *Hum Mol Genet* **18:** 723–736

Schaffar G, Breuer P, Boteva R, Behrends C, Tzvetkov N, Strippel N, Sakahira H, Siegers K, Hayer-Hartl M, Hartl FU (2004) Cellular toxicity of polyglutamine expansion proteins: mechanism of transcription factor deactivation. *Mol Cell* **15:** 95–105

Schilling G, Wood JD, Duan K, Slunt HH, Gonzales V, Yamada M, Cooper JK, Margolis RL, Jenkins NA, Copeland NG, Takahashi H, Tsuji S, Price DL, Borchelt DR, Ross CA (1999) Nuclear accumulation of truncated atrophin-1 fragments in a transgenic mouse model of DRPLA. *Neuron* **24:** 275–286

Shen Y, Lee G, Choe Y, Zoltewicz JS, Peterson AS (2007) Functional architecture of atrophins. *J Biol Chem* **282:** 5037–5044

Tanoue T, Takeichi M (2005) New insights into Fat cadherins. *J Cell Sci* **118:** 2347–2353

Tapon N, Harvey KF, Bell DW, Wahrer DC, Schiripo TA, Haber DA, Hariharan IK (2002) salvador Promotes both cell cycle exit and apoptosis in Drosophila and is mutated in human cancer cell lines. *Cell* **110:** 467–478

Taylor JP, Taye AA, Campbell C, Kazemi-Esfarjani P, Fischbeck KH, Min KT (2003) Aberrant histone acetylation, altered transcription, and retinal degeneration in a Drosophila model of polyglutamine disease are rescued by CREB-binding protein. *Genes Dev* **17:** 1463–1468

Vilhais-Neto GC, Maruhashi M, Smith KT, Vasseur-Cognet M, Peterson AS, Workman JL, Pourquie O (2010) Rere controls retinoic acid signalling and somite bilateral symmetry. *Nature* **463:** 953–957

Wang L, Rajan H, Pitman JL, McKeown M, Tsai CC (2006) Histone deacetylase-associating Atrophin proteins are nuclear receptor corepressors. *Genes Dev* **20:** 525–530

Williams AJ, Paulson HL (2008) Polyglutamine neurodegeneration: protein misfolding revisited. *Trends Neurosci* **31:** 521–528

Wood JD, Nucifora Jr FC, Duan K, Zhang C, Wang J, Kim Y, Schilling G, Sacchi N, Liu JM, Ross CA (2000) Atrophin-1, the dentato-rubral and pallido-luysian atrophy gene product, interacts with ETO/MTG8 in the nuclear matrix and represses transcription. *J Cell Biol* **150:** 939–948

Xu H, Lee SJ, Suzuki E, Dugan KD, Stoddard A, Li HS, Chodosh LA, Montell C (2004) A lysosomal tetraspanin associated with retinal degeneration identified via a genome-wide screen. *EMBO J* **23:** 811–822

Zhang S, Xu L, Lee J, Xu T (2002) Drosophila atrophin homolog functions as a transcriptional corepressor in multiple developmental processes. *Cell* **108:** 45–56

Zoltewicz JS, Stewart NJ, Leung R, Peterson AS (2004) Atrophin 2 recruits histone deacetylase and is required for the function of multiple signaling centers during mouse embryogenesis. *Development* **131:** 3–14

